Available online at www.sciencedirect.com

ScienceDirect

Procedia CIRP 42 (2016) 439 – 443

www.elsevier.com/locate/procedia

18th CIRP Conference on Electro Physical and Chemical Machining (ISEM XVIII)

Tribological Performance of Laser Patterned Cemented Tungsten Carbide Parts

S.Fang[a,b], T.Herrmann[c], A.Rosenkranz[d], C.Gachot[d], F.G.Marro[b], F.Mücklich[d], L.Llanes[b], D.Bähre[a]

[a]*Institute of Production Engineering, Saarland University, 66123 Saarbrücken, Germany*
[b]*CIEFMA – Dept. Materials Science and Metallurgical Engineering, Universitat Politècnica de Catalunya, 08028 Barcelona,Spain*
[c]*Photonik-Zentrum Kaiserslautern e.V., 67663 Kaiserslautern, Germany*
[d]*Institute of Functional Materials, Saarland University, 66123 Saarbrücken, Germany*

* Shiqi Fang. Tel.: +49 (0)681 302 4688; fax: +49 (0)681 302 4858. *E-mail address:* shiqi.fang@uni-saarland.de

Abstract

Some tools for machining processes used to be guided by supporting parts while using them for cutting or abrasive machining. For instance, the guide stone is used as supporting part in the honing process, which maintains the concentricity of the rotating axis. The contact surfaces of the supporting parts should exhibit the following properties: adequate combination of hardness, toughness and wear resistance. The damage of contact surfaces can be caused by a combination of friction and adhesion, related to the weakness of surface conditions in the tribological system, e.g. asperities, debris and pores. In order to investigate the impact of the surface topography, contact surfaces of the supporting parts made of cemented tungsten carbide (WC-Co) have been treated by means of laser surface patterning (LSP). Two different surface patterns with deterministic geometries on the micro and nano scale are achieved by two distinct LSP methods: line-like patterns by Laser-Interference Metallurgy (LIMET) with ns-laser and dimples by ps-laser. Tangential force coefficients, similar to the coefficient of friction (COF) in the non-abrasive case, are measured to evaluate the impact of the surface patterns. In this paper, the LSP methods as well as the analysis of the resulting surface topography are introduced. It is found that higher friction is obtained by line-like patterns whereas dimples can efficiently reduce the friction. At low load, hydrodynamic effects are reinforced as the dimples work as lubricant reservoirs and trap wear particles, and the observation becomes less obvious at high load. Meanwhile, only slight friction augmentation is observed by line-like patterns when the load increases.

Peer-review under responsibility of the organizing committee of 18th CIRP Conference on Electro Physical and Chemical Machining (ISEM XVIII)

Keywords: Laser Surface Patterning; Tribology; Cemented Tungsten Carbid (WC-Co); Abrasive Machining Processes; Surface Integrity

1. Introduction

Since the 1960s, it has been attempted to modify the surface topography to improve the tribological performance of the contact surfaces by several machining techniques, especially to reduce the friction and improve wear resistance [1]. Cemented tungsten carbide (WC-Co) is widely used as cutting tools and supporting parts in industry. Excessive friction between the contact surfaces always produces abundant heat and diminishes the part lifecycle. It appears to be significant to minimize the friction by surface treatment. However, WC-Co is difficult to be machined by traditional shaping methods due to its hardness. Various surface treatment methods for hardmetal, such as Electrical Discharge Machining (EDM) have been employed to machine the surfaces on the micro scale. The accuracy of these methods is fairly high compared with the traditional chip-removal method [2].

During the EDM process, a great number of tiny materials are removed individually due to the electrical discharges between the two electrodes, which finally result in a homogenous material removal. However, some defects also can be induced in the affected zone, such as pores, impurities and fractures due to thermal effects. Furthermore, these

Peer-review under responsibility of the organizing committee of 18th CIRP Conference on Electro Physical and Chemical Machining (ISEM XVIII)
doi:10.1016/j.procir.2016.02.228

methods lead to non-uniform residual stresses in the surfaces [3, 4].

Compared with EDM, laser surface patterning (LSP) is a high precision surface treatment technique, which makes use of the laser pulses with adjustable energy density and pulse repetition frequency (PRF) to machine the surfaces. LSP possesses many advantages, e.g. clean, precise and short processing time. The ablation rate and precision of LSP are strongly influenced by the pulse duration, PRF, energy density and laser wavelength [5]. Due to the high intensity, melting, recrystallization, phase transformation etc., can occur on the micro and nano scale. Thermal effects can be efficiently reduced when the pulse duration is shortened, e.g. ps-pulses have less thermal impact than ns-pulses of identical fluence. Due to less thermal effects, ps-laser results in less surface damage [6, 7].

Laser-Interference Metallurgy (LIMET) is a process, where two or three pulsed laser beams with the same PRF are superimposed on the target surface [8, 9]. By means of LIMET, it is possible to produce periodic surface patterns with dimensions on the sub sub-micron level up to micrometers, depending on the angle between the interfering beams and the thermophysical properties of the materials involved.

It is the objective of this study to introduce the fabrication methods of two different patterns with defined geometries on WC-Co surfaces by means of LSP. Surface integrity is characterized in terms of geometry. The first results related to the tribological performances will be presented.

2. Experiments

2.1. Material properties

The WC-Co hardmetal (Table 1) is selected as test sample. This hardmetal has a grain size of 20 μm and contains 14% Cobalt and 14% Nickel as binder. The hardness of the hardmetal is 610HV30, i.e. it is a relatively soft hardmetal.

Table 1. WC-Co hardmetal properties.

Material	WC-Grain Size (μm)	Co (%)	Ni (%)	Density (g/cm³)	Hardness (HV30)
VN77	20	14	14	12.82	610

2.2. LSP characteristics

The mechanism of laser-matter interaction is mainly determined by the pulse duration. When the laser pulse duration is in the range of 10 ps and below, the pulse duration is usually shorter than the heat diffusion time. Therefore, the deposited heat cannot move away and there is only a local temperature rise resulting in material phase transformations (melting and vaporisation) [10]. The difference of the Co and WC melting points denote the thermal behaviour of Co from WC in this regime. It is known that the energy intensity (fluence) less than 2.5 J/cm² is suitable to only remove Co [11]. In this case, WC grains easily break out due to melting and vaporizing of the Co glue. Two different surface patterns are produced by two types of laser installations: LIMET with ns-laser and ps-laser.

2.2.1. Line-like patterns by ns-laser

The used ns-laser is a solid state Nd: YAG source (Spectra Physics Quanta Ray Pro 290). The laser beams have a PRF of 10Hz, wavelength of 355nm, pulse duration of 10ns and fluence of 2.3 J/cm² at the machining zone (Table 2).

Table 2. Basic information of the ns-laser setup.

Laser type	Laser source	Pulse duration (ns)	Wave length (nm)	PRF (Hz)	Fluence (J/cm²)
ns-laser	Nd: YAG	10	355	10	2.3

Special configurations of the laser beam trajectories are necessary to obtain the line-like pattern with defined geometry in LIMET. Fig. 1 shows the trajectory of the laser beams: they are produced by the Nd: YAG laser source, focused by a lens, then split equally by a beam splitter. The sub-beams are reflected by the mirrors respectively and finally interfered on the target surface.

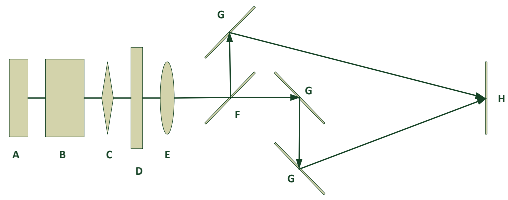

A: Laser source	C: Power meter	E:Lens	G:Mirror
B: Attenuator	D: Shutter	F:Beam splitter	H:Sample

Fig. 1. LIMET experimental setup

The superposition of the two sub-beams leads to interference resulting in a line-like pattern. Two parameters are used to describe the pattern geometry: periodicity, defined as the distance between two adjacent peaks or valleys, and height, defined as the distance between the peak and its adjacent valley. The periodicity is defined by the trajectory of the laser beams and can be obtained by Equation (1) [8]:

$$P = \frac{\lambda}{2\sin\left(\frac{\theta}{2}\right)} \quad (1)$$

λ: Laser wavelength
θ: Angle between two sub-beams
P: Calculated periodicity

Table 3 shows the experimental parameters of the ns-laser setup. Based on the listed parameters, the periodicity is calculated to be 11.3 μm. The removed material volume is mainly dependent on the absorption of the laser beam energy [5]. It means that the depth of the line-like pattern depends on the pulse energy and pulse number. The correlation between the removed material volume and the absorbed energy is not discussed in this paper.

Table 3.Experimental parameters of the ns-laser setup

λ (nm)	d (cm)	Lens (mm)	θ (°)
355	2.2	1000	1.8

2.2.2. *Dimples by ps-laser*

The ultrafast-laser machining (Table 4) with a picosecond laser system (HYPER25 Coherent Kaiserslautern GmbH) has been employed to fabricate dimples on the WC-Co surfaces. The picosecond laser system is mounted on a high precision 5-axis laser micromachining system (GL.5, GFH GmbH), which allows for a position accuracy of ±1µm and maximum axis speeds of 2m/s. The used laser PRF is 200 kHz, the wavelength was set to 532 nm, and the pulse duration is 10 ps. The fluence is 0.5 J/cm² at the machining zone.

Table 4. Laser- and process parameters using the ps-laser system

Laser type	Laser source	Pulse duration (ps)	Wave length (nm)	PRF (Hz)	Fluence (J/cm²)
ps-laser	HYPER25	10	532	200K	0.5

Due to the accuracy of the machining system, the surface patterns can be produced precisely. The dimple intervals in X and Y directions are set to be 500 µm, the feed rate is 1m/s.

2.3. *Friction tests*

The workbench (Fig. 2) is designed similar to an external honing process and allows for the study of the force evolution in the relative motion between a single tool and workpiece. The three orthogonal forces F_n, F_t and F_o are measured by the force measurement platform. F_n is the normal load applied on the contact surface, F_t is the tangential force resulted from the rotation and F_o is resulted from oscillation movement. In order to coincide with the workpiece surface, the tool surface has been machined to be curved prior to LSP. The ratio between F_n and F_t is defined as tangential force coefficient µ [12, 13]. The force coefficient, similar to the coefficient of friction (COF) in the non-abrasive case [14], is obtained by Equation (2):

$$\mu = \frac{F_t}{F_n} \tag{2}$$

Line-like patterns and dimples are tested under same conditions (Table 5) in order to observe the tribological performances. The workpiece has a rotation speed of 500 min^{-1}, corresponding with a velocity of about 40 m/min, and an oscillation speed of 1000 mm/min. The velocity is close to the industrial honing processes. For each test, the tool has 2 µm feed to the rotating workpiece, which oscillates 10 times in every 1µm feed. Normal loads are applied from 15 N to 70 N, corresponding to pressures from 0.25 MPa to 1.2 MPa on the contact surfaces. A synthetic oil (suitable for high-alloy and hardened steels with a kinematic viscosity υ of 5 mm²/s at 40°C) is used as lubricant.

Table 5. Machine configuration

Rotation speed (rpm)	Oscillation speed (mm/min)	Oscillation number/feed	Feed (µm)	Lubrication viscosity (mm²/s)
500	1000	10	2	5

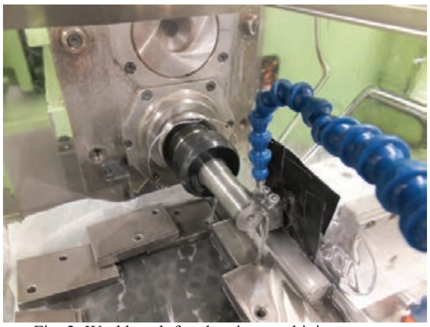

Fig. 2. Workbench for abrasive machining process

3. Surface topography

The surface topography of the two surface patterns is assessed by the Laser Scanning Microscopy (LSM) in 3 dimensions. Three important geometrical properties of the line-like patterns, which cover the entire surface in square arrangement, are investigated (Fig. 3): periodicity, height, and peak angle. Meanwhile, three important geometrical properties of the dimples are investigated (Fig. 4): interval, defined as the distance between two adjacent dimple centers; depth, defined as the distance between the dimple surface and its bottom, and dimple diameter.

a

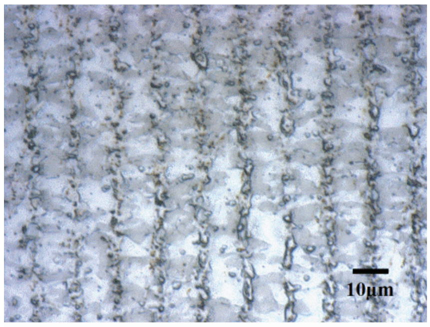

b

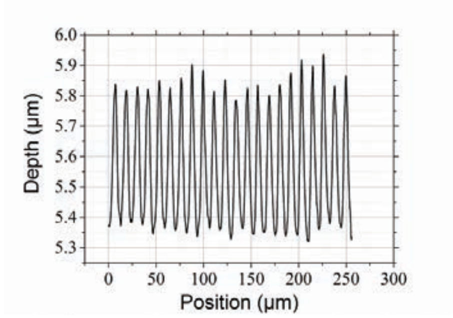

Fig. 3. Geometrical properties of the line-like patterns: a) periodicity, b) cross section profile

The line-like patterns have a periodicity of 11.8 µm, height of 0.6 µm and angle of 7.5°C. The dimples have an interval of 503.2 µm, depth of 3.8 µm and diameter of 51.3 µm.

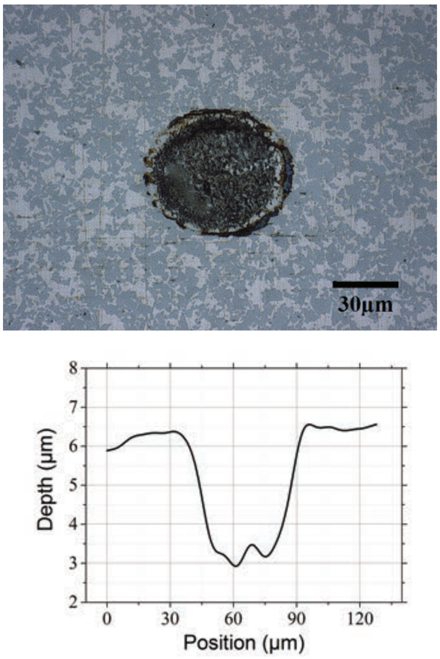

Fig. 4. Geometrical properties of the dimples: a) single dimple, b) cross section profile

4. Tribological performances

Fig. 5 shows the analysis of the COFs for the two surface patterns and a polished reference under lubricated conditions with different normal loads. The tribological performance of the two patterns varies from each other. Higher friction is obtained with line-like patterns. As the contact pressure increases, the COFs of both patterns also increase. However, the dimples have an increase with greater magnitude than the line-like patterns. Compared with the polished surface, line-like patterns show higher friction and dimples diminish remarkably the friction.

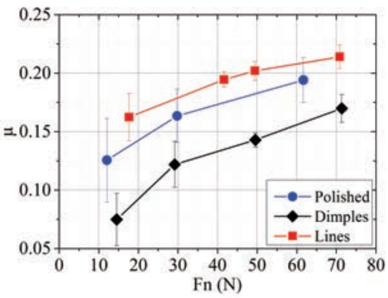

Fig. 5. Analysis of the COF for line-like patterns and dimples as a function of the normal loads

In terms of line-like patterns, the micro-asperities increase the surface roughness, which is harmful for the construction of full fluid lubrication [15]. The asperities will increase the amount of solid-solid contact. This explains the friction augmentation compared with the polished surface. In these experiments, the line-like patterns are oriented parallel to the rotation direction, which is favorable for the formation of the lubricant channels (Fig. 6). The lubricant channels connect the high pressure regions and low pressure regions, and conduct the lubricant to surrounding areas [16, 17]. In addition, the discontinuities of the line-like patterns facilitate the lubricant flow from the channels to the contact area. The lubricant channel effects are more significant under higher contact pressures [18], and this could explain why the friction by the line-like patterns is not as much as the dimples when the load increases.

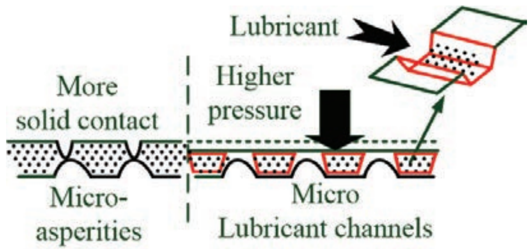

Fig. 6. Schematic diagram of the line-like pattern interfaces

In terms of dimples, two observations can be made: lower friction is attained compared with other patterns, and the friction reduction at high load is not as remarkable as that at low load. The observations can be explained by two aspects. On the one hand, the dimples act as the reservoirs in the tribological systems (Fig. 7). The reservoirs can trap the wear particles to prevent from solid-solid contact [19]. On the other hand, the reservoirs form the microcirculation of the lubricants which generates local pressure. The produced pressure is in favour to increase the thickness of the lubrication film and improve the load-carrying capacity [1, 20]. Consequently, hydrodynamic effects are enhanced to ameliorate the frictional conditions. However, the hydrodynamic effects are less pronounced at high load [15, 21], owing to the fact that full lubrication is more difficult to establish due to the absence of the lubricant channels which help redistribute the lubricant [16]. Hence the friction of the dimples has an obvious rise when the load increases.

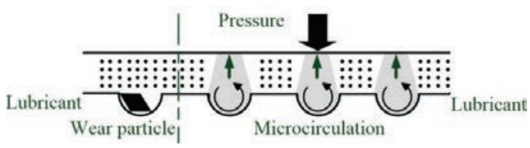

Fig. 7. Schematic diagram of the lubrication microcirculation in the dimples interfacial reaction

5. Conclusion

- Line-like patterns and dimples with defined dimensions on the WC-Co hardmetal surfaces are produced by LIMET and ultrafast-laser machining, respectively. The LIMET technique allows the fabrication of the line-like patterns with a periodicity 11.8 μm and height of 0.6 μm. The combination of the ps-laser and micromachining system offers high precision and efficiency, which is beneficial for the industrial application.
- The surface geometry assessments show that the geometries of line-like patterns and dimples correspond to the initial design.
- The friction tests indicate that the dimples can efficiently reduce the COF and expand the hydrodynamic effects. Higher friction is obtained by line-like patterns compared with polished surfaces, and only slight friction augmentation is observed by line-like patterns when the load increases.

Acknowledgements

The work was carried out within the framework of Erasmus DocMASE programme which is funded by the European Union as well as partly by the Spanish MINECO (Grant No.MAT 2012-34602). The authors are also grateful to the support and encouragement of the Photonik-Zentrum Kaiserslautern and to the material providing by Saar-Hartmetall und Werkzeuge GmbH.

References

[1] D.B. Hamilton, J.A Walowit, C.M. Allen. A theory of lubrication by micro irregularities. Wear. 1967;10(5):412.
[2] Casas B, Wiklund U, Hogmark S, Llanes L. Adhesion and abrasive wear resistance of TiN deposited on electrical discharge machined WC-Co cemented carbides. Wear. 2008;265(3-4):490–6.
[3] M'Saoubi R, Outeiro JC, Chandrasekaran H, Jr. OWD, Jawahir IS. A review of surface integrity in machining and its impact on functional performance and life of machined products. Int J Sustain Manuf. 2008;1(1/2):203–36.
[4] Llanes L, Mart E, Ida E, Casas B, Esteve J. Influence of electrical discharge machining on the sliding contact response of cemented carbides. International Journal. 2001. p. 35–40.
[5] Dumitru G, Lüscher B, Krack M, Bruneau S, Hermann J, Gerbig Y. Laser processing of hardmetals: Physical basics and applications. Int J Refract Met Hard Mater. 2005;23(4-6 SPEC. ISS.):278–86.
[6] Fatima a., Whitehead DJ, Mativenga PT. Femtosecond laser surface structuring of carbide tooling for modifying contact phenomena. Proc Inst Mech Eng Part B J Eng Manuf [Internet]. 2014
[7] Chichkov BN, Momma C, Nolte S, von Alvensleben F, Tünnermann a. Femtosecond, picosecond and nanosecond laser ablation of solids. Appl Phys A Mater Sci Process. 1996;63(2):109–15.
[8] Mücklich F, Lasagni a., Daniel C. Laser interference metallurgy - Periodic surface patterning and formation of intermetallics. Intermetallics. 2005;13(3-4):437–42.
[9] Duarte M, Lasagni A, Giovanelli R, Narciso J, Louis E, Mücklich F. Increasing lubricant film lifetime by grooving periodical patterns using laser interference metallurgy. Adv Eng Mater. 2008;10(6):554–8.
[10] Yao YL, Chen H, Zhang W. Time scale effects in laser material removal: a review. Int J Adv Manuf Technol. 2005;26(5-6):598–608.
[11] Li T, Lou Q, Dong J, Wei Y, Liu J. Selective removal of cobalt binder in surface ablation of tungsten carbide hardmetal with pulsed UV laser. Surf Coatings Technol. 2001;145(1-3):16–23.
[12] Saljé E, von See M. Process-Optimization in Honing. CIRP Ann - Manuf Technol. 1987;36(1):235–9.
[13] H.-W. Hoffmeister, B. Menze. Einsatz von Sensorik beim Honen und Regelung von Honprozessen. Jahrbuch Schleifen, Honen, Läppen und Polieren. 2004. p.61.
[14] Marinescu I, Rowe B, Dimitrov B, Inasaki I. Tribology of Abrasive Machining Processes. Journal of Manufacturing Science and Engineering. 2004. p. 148-154.
[15] Yuan S, Huang W, Wang X. Orientation effects of micro-grooves on sliding surfaces. Tribol Int [Internet]. Elsevier; 2011;44(9):1047–54.
[16] Steinhoff K, Rasp W, Pawelski O. Development of deterministic-stochastic surface structures to improve the tribological conditions of sheet forming processes. Journal of Materials Processing Technology. 1996. p. 355–61.
[17] Pettersson U, Jacobson S. Friction and wear properties of micro textured DLC coated surfaces in boundary lubricated sliding. Tribol Lett. 2004;17(3):553–9.
[18] Costa HL, Hutchings IM. Hydrodynamic lubrication of textured steel surfaces under reciprocating sliding conditions. Tribol Int. 2007;40(8):1227–38.
[19] Suh NP, Mosleh M, Howard PS. Control of friction. Wear 1994;175:151–8.
[20] Nakano M, Korenaga A, Korenaga A, Miyake K, Murakami T, Ando Y, et al. Applying micro-texture to cast iron surfaces to reduce the friction coefficient under lubricated conditions. Tribol Lett. 2007;28(2):131–7.
[21] Wang X, Liu W, Zhou F, Zhu D. Preliminary investigation of the effect of dimple size on friction in line contacts. Tribol Int. 2009;42(7):1118–23.